Thermal vector potential theory of magnon-driven magnetization dynamics

Gen Tatara
RIKEN Center for Emergent Matter Science (CEMS), 2-1 Hirosawa, Wako, Saitama 351-0198, Japan
(Received 7 May 2015; published 3 August 2015)

Thermal vector potential formulation is applied to study the thermal dynamics of magnetic structures for insulating ferromagnets. By separating the variables of the magnetic structure and the magnons, the equation of motion for the structure, including spin-transfer effect because of thermal magnons, is derived for the cases of a domain wall and a vortex. The magnon current is evaluated based on the linear response theory with the thermal vector potential representing the temperature gradient. The velocity of a domain wall when driven by thermal magnons exhibits a strong temperature dependence unlike the case of an electrically driven domain wall in metals.

DOI: 10.1103/PhysRevB.92.064405 PACS number(s): 72.20.Pa, 75.60.Ch, 75.30.Ds

I. THERMAL EFFECTS IN SPINTRONICS

The manipulation of magnetization and spin current without an applied magnetic field is a key issue in spintronics technology. For metallic ferromagnets, electric current has been shown to be very useful for switching the magnetization and for driving magnetic domain walls using current-induced spin-transfer torques proposed by Berger [1,2] and Slonczewski [3]. Moreover, metallic systems have been extensively studied for spin current manipulation such as for direct and inverse spin Hall effects [4,5]. In addition to metallic magnets, insulating ferrimagnets, such as yttrium iron garnet (YIG), are also expected to be useful spintronics materials [6] because of their weak spin relaxation effects as represented by the small Gilbert damping parameter, α. Although the use of electric current is not applicable to insulators, extensive studies recently revealed that manipulation of magnetization of YIG is possible using several different methods, such as a temperature gradient [7] and sound waves [8]. Thermal methods are particularly important for realizing novel thermoelectric materials based on magnetic materials [9,10], which are expected to be useful for devices with low energy consumption.

Recently, thermally driven domain wall motion in a YIG film was observed [11]. The domain wall was found to move to the hotter side of the system with the speed of about 2×10^{-4} m/s for an applied temperature gradient of $\nabla T = 20$ K/mm. The direction of the motion is counterintuitive but consistent with the spin-transfer effect of spin waves (magnons) [12,13]. In fact, magnons excited around the wall are pushed by the temperature gradient to the colder side and transfer spin angular momentum opposite to the local magnetization, resulting in domain wall motion toward the hotter side. This motion was studied from a thermodynamic viewpoint by Wang [14] using numerical evaluation of the entropy and free energy because of the magnons around the wall. It was concluded that the wall motion to the hotter side is consistent with the minimization of free energy when the entropy because of magnons is considered. Thermal motion of domain walls toward the colder end was observed in metallic ferromagnets in 1986 [15]. While wall-entropy force proportional to ∇T was suggested as a possible mechanism [16,17], this behavior can be simply explained by the spin-transfer torque induced by the thermally driven conduction electrons. In 2010, Hals *et al.* [18] studied a thermal motion of a domain wall in GaMnAs, including the effect of thermally induced force calculated by scattering theory; The spin transfer effect caused by magnons was not considered.

Domain walls under a temperature gradient were numerically studied by solving the Landau-Lifshitz-Gilbert (LLG) equation for spins in Ref. [12], in which the effect of temperature was modeled as a random magnetic field satisfying the fluctuation-dissipation theorem. The results indicated that the behavior of the wall is essentially the same as in the electric-current-driven case [19–21]. For instance, a sliding motion with a constant tilting angle occurs for the case of a low driving force or for large damping, and the tilting angle becomes time-dependent, resulting in a screw-like motion when the driving force exceeds a threshold value corresponding to Walker's breakdown field. Moreover, the LLG approach was used to study the motion of magnetic skyrmions [22], which turned out to move to the hotter region in the same manner as domain walls with a velocity inversely proportional to the Gilbert damping parameter, α. The numerical results were explained by the Brownian motion of the skyrmions driven by thermal random magnetic field and the spin-transfer effect from thermal spin waves. The spin wave spin-transfer effect contributing to the motion toward the hotter side is proportional to $\nabla T/\alpha$, while the velocity because of the Brownian motion, which pushes the skyrmions to the colder side, is proportional to $\alpha\nabla T$; thus, it is negligible for small α.

The approach describing thermal effects using a random magnetic field was also employed in Refs. [23,24]. In Ref. [23], the force on the domain wall induced by thermal magnons in the presence of Gilbert damping was calculated and the effective nonadiabaticity parameter for a thermal force β_T was found to be $\beta_T \sim \frac{d}{2}\alpha$, where d is the dimension. The temperature dependence of the exchange stiffness resulted in another magnon-induced force (so-called entropic force) proportional to the gradient of magnon density [24,25]. Magnon reflection by the wall was extensively studied in Ref. [26], and the reflection was shown to exert a force on the domain wall in the same manner as in the case of electron reflection discussed in Ref. [27]. The reflection rate was calculated based on the Landauer-Büttiker formula and the temperature dependence of the force was investigated.

This study aims to present a consistent theoretical formalism for magnetization dynamics induced by thermally driven magnons based on the linear response theory. The expression for magnon spin-transfer torque is derived in a rigorous mathematical manner using a unitary transformation in spin space, and the magnon current is evaluated quantum mechanically using the linear response theory. Therefore, the torque caused by thermal magnons is treated in the same manner as in the case driven by an electric current [21]. We have not discussed the magnon force described in Refs. [23,26]; however, a force because of the nonadiabaticity can be incorporated into the present framework in a straightforward manner.

II. LUTTINGER'S FORMULATION OF THERMAL TRANSPORT

Theories of thermally driven magnetic systems have, to date, been mostly phenomenological [11,17,28] or numerical [12,22] and have lacked a microscopic viewpoint. The reason for this is obvious: the temperature gradient appears to be impossible to integrate into a linear response theory or field-theoretical methods in a straightforward manner because its effect is not described by a microscopic interaction Hamiltonian. However, this difficulty was removed for electron transport phenomena by Luttinger in 1964 [29]. He introduced a fictitious scalar field called a "gravitational" potential, Ψ, which couples to the local energy density, $\mathcal{E}$, by an interaction Hamiltonian:

$$H_{\rm L} = \int d^3 r \Psi \mathcal{E}. \quad (1)$$

It was argued that Ψ satisfies $\nabla\Psi = \frac{\nabla T}{T}$ and that a linear response theory (Kubo formula) is applicable to the thermally driven case by considering the correlation functions of the energy current density. Multiple studies based on the "gravitational" potential formalism have been conducted on electron transport [30–37], quantum dots [38], magnon transport [39–41], and thermal torques [42]. At the same time, it has been observed that a naive application of the Kubo formula may result in wrong thermal coefficients [30,31,35,42].

An alternative Landauer-like approach of connecting locally equilibrium systems at different temperatures may be used for studies of thermal transport [43,44]. It was shown in Ref. [43] that the obtained transport coefficients do not display an unphysical divergence because they are only caused by the electrons at the Fermi energy level. A quantum kinetic equation approach was employed in Refs. [33,34] to study electron correlation effects; however, a completely quantum mechanical description based on the linear response theory would be more widely applicable and highly useful.

Approaches to extract correct results based on the "gravitational" potential formalism were explored in some previous studies [30,35,42]. For thermally induced electron transport, Smrcka and Streda performed a calculation of the thermal Hall effect in the presence of an applied magnetic field based on Luttinger's method [30,31]. They rewrote Luttinger's interaction, $\Psi\mathcal{E}$, as $-\mathcal{E}\boldsymbol{r}\cdot\nabla\Psi$ using integration by parts and performed a perturbative expansion with respect to a physical force proportional to $\nabla\Psi = \nabla T/T$. However, this analysis is based on an expansion with respect to an interaction proportional to an unbounded operator, $\boldsymbol{r}$; thus, the results may not always be convincing. Recent studies of thermal magnons are based on the same approach [41]. Qin *et al.* reported that a naive application of Luttinger's approach for the thermal Hall effect leads to a unphysical divergence at $T \to 0$ and that this divergence is caused by an equilibrium rotational electron current induced when the time-reversal invariance is broken by the magnetic field [35]. They demonstrated that the correct nonequilibrium response is obtained if one subtracts the equilibrium current before applying the "gravitational" potential.

The case of a thermally induced torque in ferromagnetic metals was studied in detail by Kohno *et al.* [42]. They calculated the nonequilibrium torque on the magnetization generated by the conduction electrons when a temperature gradient is applied and found that unphysical divergence arises for a straightforward application of Luttinger's approach. Moreover, they demonstrated that the divergence is caused by the equilibrium torque describing the exchange interaction between the magnetization and that this equilibrium contribution must be removed when treating the nonequilibrium torque.

III. VECTOR POTENTIAL FORMULATION

Recently, in Ref. [45], the problems associated with Luttinger's formalism were reported to be caused by the "gravitational" potential coupling to the total energy density, thus modifying the equilibrium properties in addition to inducing the nonequilibrium response. It was shown that the role of diamagnetic current, which is essential for removing unphysical equilibrium (nondissipative) contribution from transport coefficients [35,46], is not seen directly in the scalar potential formalism. Instead of a scalar potential formalism, a vector potential formalism to describe thermally induced transport was developed in Refs. [45,47]. In Ref. [47], Shitade demonstrated using the analogy of general relativity [48] that if an invariance under time translation is locally imposed, a vector potential arises from Luttinger's scalar potential and they are described by a gauge invariant theory. He applied his model to describe the thermal Hall effect of noninteracting electrons and showed that the results satisfy the Wiedemann-Franz law; however, the origin of the invariance under local time translation was not explained. In Ref. [45], the vector potential was introduced by rewriting Luttinger's Hamiltonian for "gravitational" potential using the law of energy conservation in the static (dc) limit of the temperature gradient and was discussed in the context of the entropy force. Because the thermal vector potential couples to the energy current, it only generates excitations and does not alter equilibrium contributions. Thus, the vector potential representation enables straightforward linear response calculations for thermal dynamics on the same footing as in the electric field-driven case. The unphysical equilibrium contributions are indeed automatically canceled by "diamagnetic" currents associated with the vector potential. A possibility of vector potential description was briefly mentioned in Ref. [49] while discussing magnon-drag thermoelectric effects.

The vector potential form of the interaction Hamiltonian describing the thermal effect is

$$H_{A_T} \equiv -\int d^3 r\, \boldsymbol{j}_{\mathcal{E}}(\boldsymbol{r},t)\cdot \boldsymbol{A}_T(t), \quad (2)$$

where $\boldsymbol{j}_\mathcal{E}$ is the energy current density and $\boldsymbol{A}_T(t)$ is the thermal vector potential, which satisfies

$$\partial_t \boldsymbol{A}_T(\boldsymbol{r},t) = \nabla\Psi(\boldsymbol{r},t) = \frac{\nabla T}{T}. \tag{3}$$

The interaction Hamiltonian of Eq. (2) was used to describe thermally induced longitudinal transport and the Hall effect of noninteracting electrons [45,47].

In this study, we apply this formalism to study thermally induced magnetization dynamics. The vector potential representation turns out to be highly useful, enabling a clear description of thermal torque in the same manner as that for the electrically driven case [21].

IV. ENERGY CURRENT OF LOCALIZED SPINS

To study thermal transport using Eq. (2), the expression for the energy current density must be derived. Following Ref. [45], we perform the derivation quantum mechanically using the law of energy conservation [50]:

$$\dot{\mathcal{E}} + \nabla\cdot \boldsymbol{j}_\mathcal{E} = 0. \tag{4}$$

We consider a case of a ferromagnet with an easy-axis and a hard-axis magnetic anisotropy energies. The Hamiltonian describing the localized spin $\boldsymbol{S}$ is $H \equiv \int d^3r\mathcal{E}$, in which

$$\mathcal{E} = \frac{1}{2a^3}[J(\nabla \boldsymbol{S})^2 - K(S_z)^2 + K_\perp(S_y)^2] \tag{5}$$

is the energy density; J, $K(>0)$, and $K_\perp(\geqslant 0)$ represent the energy of the exchange interaction, the easy-axis anisotropy, and the hard-axis anisotropy, respectively; and a is the atomic lattice constant. The energy current density in this case is obtained as (see Sec. I for the derivation)

$$j_{\mathcal{E},i} = -\frac{J}{a^3}\nabla_i \boldsymbol{S}\cdot\dot{\boldsymbol{S}}. \tag{6}$$

Thermally driven dynamics of the spin structure is calculated below as a linear response to the interaction H_{A_T} [Eq. (2)] with the energy current density of Eq. (6).

V. SEPARATION OF VARIABLES

To perform the calculation of thermally driven magnetization dynamics, we separate the collective degrees of freedom describing a classical magnetization structure and fluctuation (magnons or spin waves) around the structure. The directions of the localized spins for the classical solution are represented using polar angles $\theta(\boldsymbol{r},t)$ and $\phi(\boldsymbol{r},t)$, which are defined by $\boldsymbol{S} = S(\sin\theta\cos\phi, \sin\theta\sin\phi, \cos\theta)$ ($S \equiv |\boldsymbol{S}|$). Then, the magnon excitation around the structure is represented using the Holstein-Primakov boson defined with respect to the local quantization axis along $\boldsymbol{S}$. The localized spin vector $\boldsymbol{S}$ is thus represented as

$$\boldsymbol{S} = U(\boldsymbol{r},t)\widetilde{\boldsymbol{S}} \equiv U(\boldsymbol{r},t)(S\hat{\boldsymbol{z}} + \delta\boldsymbol{s}), \tag{7}$$

where $\hat{\boldsymbol{z}}$ is the unit vector along the z axis; U is a 3×3 unitary matrix describing a rotation of a vector $\hat{\boldsymbol{z}}$ to the direction $\boldsymbol{S}$, i.e., $\widetilde{\boldsymbol{S}} \equiv S\hat{\boldsymbol{z}} + \delta\boldsymbol{s}$; and $\delta\boldsymbol{s}$ represents the fluctuation. The unitary matrix is chosen as follows [51]:

$$U = \begin{pmatrix} \cos\theta\cos\phi & -\sin\phi & \sin\theta\cos\phi \\ \cos\theta\sin\phi & \cos\phi & \sin\theta\sin\phi \\ -\sin\theta & 0 & \cos\theta \end{pmatrix}, \tag{8}$$

and the fluctuation is represented in terms of annihilation and creation operators for the magnon (the Holstein-Primakov boson), b and $b^\dagger$, as follows [52]:

$$\delta\boldsymbol{s} = \begin{pmatrix} \gamma(b^\dagger + b) \\ i\gamma(b^\dagger - b) \\ -b^\dagger b \end{pmatrix}, \tag{9}$$

where $\gamma \equiv \sqrt{\frac{S}{2}}$. We neglect the terms that are third- and higher-order in boson operators.

The unitary transformation modifies the derivatives of spin as ($\mu = t,x,y,z$)

$$\partial_\mu \boldsymbol{S} = U(\partial_\mu + iA_{U,\mu})\widetilde{\boldsymbol{S}}, \tag{10}$$

where

$$A_{U,\mu} \equiv -iU^{-1}\nabla_\mu U \tag{11}$$

is the spin gauge field represented by a 3×3 matrix. Explicitly, the spin gauge field is expressed by

$$A_{U,\mu} = -i\nabla_\mu\theta\begin{pmatrix} 0 & 0 & 1 \\ 0 & 0 & 0 \\ -1 & 0 & 0 \end{pmatrix} - i\nabla_\mu\phi\begin{pmatrix} 0 & -\cos\theta & 0 \\ \cos\theta & 0 & \sin\theta \\ 0 & -\sin\theta & 0 \end{pmatrix}. \tag{12}$$

The energy current density [Eq. (6)] is then

$$\begin{aligned} j_{\mathcal{E},i} &= -\frac{J}{a^3}\widetilde{\boldsymbol{S}}(\overleftarrow{\partial_t} - iA_{U,t})(\nabla_i + iA_{U,i})\widetilde{\boldsymbol{S}} \\ &= -\frac{J}{a^3}\bigg(S^2[(\nabla_i\theta)\dot{\theta} + \sin^2\theta(\nabla_i\phi)\dot{\phi}]\bigg(1 - \frac{1}{S}b^\dagger b\bigg) + S[\dot{b^\dagger}(\nabla_i b) + (\nabla_i b^\dagger)\dot{b}] \\ &\quad + S\{-i\cos\theta[\dot{\phi}(b^\dagger\overleftrightarrow{\nabla} b) + (\nabla_i\phi)(b^\dagger \overleftrightarrow{\partial_t} b)] + 2\cos^2\theta(\nabla_i\phi)\dot{\phi}b^\dagger b\} \\ &\quad + S\gamma\{-i\cos\theta[\dot{\theta}(\nabla_i\phi) + (\nabla_i\theta)\dot{\phi}](b^\dagger - b) + (\dot{\theta} + i\sin\theta\dot{\phi})(\nabla_i b^\dagger) + (\dot{\theta} - i\sin\theta\dot{\phi})(\nabla_i b) \\ &\quad + (\nabla_i\theta + i\sin\theta\nabla_i\phi)(\dot{b^\dagger}) + (\nabla_i\theta - i\sin\theta\nabla_i\phi)(\dot{b})\}\bigg). \end{aligned} \tag{13}$$

The first term,

$$j^{(s)}_{\mathcal{E},i} \equiv -\frac{J}{a^3}S^2[(\nabla_i\theta)\dot{\theta} + \sin^2\theta(\nabla_i\phi)\dot{\phi}]\left(1 - \frac{1}{S}b^\dagger b\right), \quad (14)$$

is the energy current carried by the magnetization structure, and

$$j^{(m)}_{\mathcal{E},i} \equiv -\frac{JS}{a^3}[\dot{b}^\dagger(\nabla_i b) + (\nabla_i b^\dagger)\dot{b}] \quad (15)$$

is the contribution of the magnons. The temperature gradient appears to act on the magnetization structure as well as on the spin waves; however, we must be careful because Eq. (14) may contain a steady-state contribution that does not contribute to the thermally excited response (see Sec. VII). The mixed contributions in Eq. (13), in which the energy current is carried by both the spin texture and the magnon, turn out to be second order in the temperature gradient and are therefore neglected. Similarly, the last contributions linear in the magnon operators are neglected. Thus, it is sufficient to consider the two energy currents given by Eqs. (14) and (15) in the following analysis of the linear response regime. Neglected interactions lead to nonadiabatic corrections such as the force because of magnon reflection.

VI. MAGNON SPIN-TRANSFER EFFECT

Using Eq. (10), the exchange interaction is written as follows:

$$\frac{J}{2}\int\frac{d^3r}{a^3}(\nabla\boldsymbol{S})^2 = \frac{J}{2}\int\frac{d^3r}{a^3}(\nabla\widetilde{\boldsymbol{S}})^2 + H^{\rm st}_J, \quad (16)$$

where

$$H^{\rm st}_J \equiv -i\frac{J}{2}\int\frac{d^3r}{a^3}\widetilde{\boldsymbol{S}}^\dagger(\boldsymbol{A}_U\cdot\overleftrightarrow{\nabla})\widetilde{\boldsymbol{S}} = 4JS\int d^3r\,\boldsymbol{A}_{\rm s}\cdot\boldsymbol{j}^{(0)}_{\rm m} \quad (17)$$

represents the interaction between the spin structure and the magnons (superscript st denotes spin transfer), and the contributions that are second order in A_U are neglected. Here,

$$\boldsymbol{A}_{\rm s} \equiv \tfrac{1}{2}\cos\theta\nabla\phi \quad (18)$$

is the adiabatic component of the spin gauge field [21], and

$$\boldsymbol{j}^{(0)}_{\rm m} \equiv -\frac{i}{2a^3}(b^\dagger\overleftrightarrow{\nabla}b) \quad (19)$$

is the magnon current density without the vector potential contribution ("paramagnetic" magnon current density). As seen in Eq. (17), the magnon current couples to the adiabatic spin gauge field in a manner similar to the electric current in metals in the adiabatic regime [21,27]. Therefore, the magnon current induces the spin-transfer torque with the transferred angular momentum per area and per unit time of $4JSj_{\rm m}$ [instead of $\frac{\hbar}{e}Pj$ in the case of electric current (P is the spin polarization of the current and e is the electron charge)].

Another contribution to the interaction between the magnetization structure and the magnons is the one arising from H_{A_T} [Eq.(2)]. Using Eq. (13), the spin-transfer terms in H_{A_T} are

$$H^{\rm st}_{A_T} \equiv i\frac{J}{a^3}A_{T,i}\int d^3r[(\partial_t\widetilde{\boldsymbol{S}})A_{U,i}\widetilde{\boldsymbol{S}} + (\nabla_i\widetilde{\boldsymbol{S}})A_{U,t}\widetilde{\boldsymbol{S}}]. \quad (20)$$

Considering only the contributions that are second order in the magnon operators, Eq. (20) becomes

$$H^{\rm st}_{A_T} = 4JS\int d^3r\,\boldsymbol{A}_{\rm s}\cdot\boldsymbol{j}^{(d)}_{\rm m}, \quad (21)$$

where

$$\boldsymbol{j}^{(d)}_{\rm m} \equiv -\frac{i}{2a^3}\boldsymbol{A}_T(b^\dagger\overleftrightarrow{\partial_t}b) \quad (22)$$

is the "diamagnetic" magnon current. Thus, the total magnon spin-transfer effect is described by

$$H_{\rm ST} = 4JS\int d^3r\,\boldsymbol{A}_{\rm s}\cdot\boldsymbol{j}_{\rm m}, \quad (23)$$

where $\boldsymbol{j}_{\rm m} \equiv \boldsymbol{j}^{(0)}_{\rm m} + \boldsymbol{j}^{(d)}_{\rm m}$.

VII. DOMAIN WALL

Let us describe a domain wall based on the Hamiltonian Eq. (5). We consider a thin wire so that the magnetization structure is treated as one-dimensional, i.e., changing only in the wire direction, which we choose as the z axis. The classical solution of the equation of motion is as follows:

$$\cos\theta = \tanh\frac{z - X(t)}{\lambda}, \quad \sin\theta = \frac{1}{\cosh\frac{z-X(t)}{\lambda}}, \quad (24)$$

and $\nabla_z\phi(t) = 0$, where $\lambda \equiv \sqrt{\frac{J}{K}}$ is the thickness of the domain wall. Then, we have

$$\nabla_z\boldsymbol{S} = -\frac{S}{\lambda}\boldsymbol{e}_\theta, \quad (25)$$

where $\boldsymbol{e}_\theta \equiv (\cos\theta\cos\phi, \cos\theta\sin\phi, -\sin\theta)$.

We first demonstrate that the energy current of the wall given by Eq. (14) is an equilibrium contribution, which should not be considered. Let us first see what happens if Eq. (14) is naively applied. Neglecting the corrections of the order of S^{-1} by magnons, Eq. (14) for domain wall is

$$j^{(s)}_{\mathcal{E},i} = \delta_{i,z}\frac{JS^2}{\lambda^2a^3}\dot{X}\frac{1}{\cosh^2\frac{z-X(t)}{\lambda}}. \quad (26)$$

Then, the coupling between the domain wall and temperature gradient described by Eq. (2) becomes

$$H_{A_T} = \frac{2AJS^2}{a^3\lambda}\frac{\nabla_z T}{T}\int_0^t dt'\dot{X}(t') = N_{\rm w}\frac{JS^2}{\lambda^2}\frac{\nabla_z T}{T}X, \quad (27)$$

where $N_{\rm w} \equiv 2\lambda A/a^3$ is the number of spins in the wall (A is the cross sectional area of the system). One may be tempted to conclude that the thermal force on the wall is

$$F_T \equiv -\frac{\delta H_{A_T}}{\delta X} = -N_{\rm w}\frac{JS^2}{2\hbar\lambda^2}\frac{\nabla_z T}{T}, \quad (28)$$

but the increase of this force at lower temperatures when ∇T is fixed is unphysical [53]. The problem arises from the energy current density of Eq. (26), which indicates that the energy current increases proportionally to the wall speed $\dot{X}$. However, this energy current is a steady-state current, which does not contribute to the entropy change because the energy carried by the domain wall is not converted to heat unless the wall is annihilated. Therefore, to consider the standard experimental situation in which the wall is semimacroscopic and is not annihilated, the steady-state contribution must be subtracted from Eq. (26), resulting in a vanishing energy current for the wall. This treatment is consistent with the argument in Ref. [14]. The direct thermal force is physical if we consider an ensemble of domain walls that are allowed to be created and annihilated (see Sec. VIII).

Therefore, the thermal effect for a domain wall is caused only from the magnon interaction $H_J^{\rm st}$ [Eq. (17)]. Because $\frac{\delta A_{{\rm s},i}}{\delta\phi} = \frac{1}{2}\sin\theta\nabla_i\theta$, the force and torque induced by the magnon interaction are given by

$$F_{\rm m} \equiv -\frac{\delta H_J^{\rm st}}{\delta X} = 0,$$
$$\tau_{\rm m} \equiv \frac{\delta H_J^{\rm st}}{\delta\phi} = -\frac{2JS}{\lambda} j_{{\rm m},z}\int d^3r \frac{1}{\cosh^2\frac{z}{\lambda}} = -\frac{2N_{\rm w}JSa^3}{\lambda} j_{{\rm m},z}. \tag{29}$$

In Eq. (29), the force from the magnon disappears because here we consider a static one-dimensional domain wall neglecting wall-magnon interactions in Eq. (13) so that the magnons are in the perfect adiabatic limit [54]; i.e., magnon modes are orthogonal to the collective modes of a static one-dimensional domain wall [21]. The force from the magnons may arise when the wall is dynamic [55] or higher-dimensional and in the presence of either the dipolar interaction [56] or Gilbert damping [23]. Here, using a dimensionless parameter β_T, we phenomenologically introduce the thermal force as $F_\beta \equiv -\beta_T\frac{N_{\rm w}S}{\lambda^2}k_Ba^2\nabla_zT$. (The coefficient β_T was shown to be $\beta_T \propto \alpha$ in Refs. [23,24] and $\beta_T \propto |r|^2$ ($|r|^2$ is the magnon reflection rate) in Ref. [26].) Including this force and the thermal magnon effects, the equation of motion for the wall is then

$$\dot\phi + \alpha\frac{\dot X}{\lambda} = -\beta_T\frac{k_Ba^2}{\hbar\lambda}\nabla_zT,$$
$$\dot X - \alpha\lambda\dot\phi = \frac{K_\perp\lambda S}{2\hbar}\sin 2\phi + \frac{\lambda}{\hbar N_{\rm w}S}\tau_{\rm m} \tag{30}$$
$$= \frac{K_\perp\lambda S}{2\hbar}\sin 2\phi - \frac{2Ja^3}{\hbar}j_{{\rm m},z}.$$

Note that the magnitude of the magnon current is evaluated in Sec. IX using linear response theory with respect to H_{A_T}.

VIII. VORTEX

Let us next consider the case of a single vortex that appears in a two-dimensional submicron size disk. The Hamiltonian describing the vortex is given by

$$H = \int\frac{d^2r}{a^2}\left[\frac{J}{2}(\nabla \boldsymbol{S})^2 - \frac{K}{2}(S_z)^2\right], \tag{31}$$

and the vortex structure with a vortex number of unity is approximately represented as follows [57]:

$$\boldsymbol{S}_{\rm v}(\boldsymbol{r}) = S\left[\cos\left(\varphi + \frac{\pi}{2}c\right)\boldsymbol{e}_x + \sin\left(\varphi+\frac{\pi}{2}c\right)\boldsymbol{e}_y\right], \tag{32}$$

where $\tan\varphi = \frac{y}{x}$ and c is an integer representing chirality. Using the collective coordinates $X(t)$ and $Y(t)$ to represent the center of the vortex in two dimensions, the spin structure is $\boldsymbol{S}(\boldsymbol{r},t) = \boldsymbol{S}_{\rm v}[\boldsymbol{r} - \boldsymbol{X}(t)]$, where $\boldsymbol{X}(t) \equiv [X(t),Y(t)]$. We first consider the case where the vortex cannot be annihilated, as is for the domain wall case; here, all thermal effects then are caused by the magnons. For a uniform magnon current, the spin-transfer torque because of magnons [Eq. (17)] is written as follows:

$$H_J^{\rm st} = \frac{2J}{S^2}\int d^2r\boldsymbol{S}\cdot\left[\left(\boldsymbol{j}_{\rm m}^{(2{\rm d})}\cdot\nabla\right)\boldsymbol{S}\times\delta\boldsymbol{S}\right], \tag{33}$$

where $\delta\boldsymbol{S}$ is the change of $\boldsymbol{S}$ when the origin of $\boldsymbol{X}$ is shifted by an amount $\delta\boldsymbol{X} = (\delta X,\delta Y)$. (This representation is convenient for focusing on the physical contribution in topological quantities for spin [58].) The magnon current density $\boldsymbol{j}_{\rm m}^{(2{\rm d})}$ is the two-dimensional one ($\boldsymbol{j}_{\rm m}^{(2{\rm d})} = \boldsymbol{j}_{\rm m}L_z$ where L_z is the thickness of the system). Therefore, the force because of spin transfer is

$$F_{{\rm st},i} \equiv -\frac{\delta H_J^{\rm st}}{\delta X_i} = -\frac{2J}{S^2}\int d^2r\boldsymbol{S}\cdot[\nabla_i\boldsymbol{S}\times\nabla_j\boldsymbol{S}]j_{{\rm m},j}^{(2{\rm d})}. \tag{34}$$

This force is characterized by the topological number density of the vortex,

$$G = \frac{\hbar}{S^2}\int\frac{d^2r}{a^2}\boldsymbol{S}\cdot[\nabla_x\boldsymbol{S}\times\nabla_y\boldsymbol{S}] = \frac{2\pi\hbar S}{a^2}, \tag{35}$$

as

$$\boldsymbol{F}_{\rm st} = \frac{2Ja^2}{\hbar}\boldsymbol{G}\times\boldsymbol{j}_{\rm m}^{(2{\rm d})}, \tag{36}$$

where $\boldsymbol{G} \equiv G\hat{\boldsymbol{z}}$. The equation of motion of a vortex is then [51,57]

$$-\boldsymbol{G}\times\dot{\boldsymbol{X}} + \alpha D\dot{\boldsymbol{X}} = \boldsymbol{F}_{\rm st}, \tag{37}$$

where $D \simeq \frac{\hbar S}{a^2}\int d^2r\sin^2\theta(\nabla\phi)^2$ is a form factor for damping. The equation is written as

$$\dot{\boldsymbol{X}} + \frac{2Ja^2}{\hbar}\boldsymbol{j}_{\rm m}^{(2{\rm d})} = -\frac{\alpha D}{G^2}\boldsymbol{G}\times\dot{\boldsymbol{X}}. \tag{38}$$

Thus, the velocity is

$$\dot{\boldsymbol{X}} = -\frac{1}{1+\left(\frac{\alpha D}{G}\right)^2}\left(1 + i\sigma_y\frac{\alpha D}{G}\right)\frac{2Ja^2}{\hbar}\boldsymbol{j}_{\rm m}^{(2{\rm d})}, \tag{39}$$

where σ_y is the y component of the Pauli matrix. Then, we consider the case of a temperature gradient along the x direction. Because the magnon current is along ∇T, the vortex velocity is

$$\begin{pmatrix}\dot X\\ \dot Y\end{pmatrix} = \frac{1}{1+\left(\frac{\alpha D}{G}\right)^2}\frac{2Ja^2}{\hbar}j_{\rm m}^{(2{\rm d})}\begin{pmatrix}-1\\ \frac{\alpha D}{G}\end{pmatrix}. \tag{40}$$

A direct force term proportional to ∇_xT appears in a previous numerical simulation study of the Fokker-Planck equation performed for a skyrmion [22]. (A single skyrmion and a vortex are described by the same equation called the Thiele equation [51] and thus exhibit a response similar to applied forces.) Such a direct force arises in our formalism by considering annihilation of vortices by considering the energy current Eq. (14) as physical current contributing to the entropy production. The energy current density in this case becomes $\boldsymbol{j}_{\mathcal{E}} = \gamma_{\rm v}\dot{\boldsymbol{X}}$ ($\gamma_{\rm v}$ is a temperature-dependent coefficient), and the direct thermal force becomes

$$\boldsymbol{F}_T = -\frac{\delta H_{A_T}}{\delta \boldsymbol{X}} = \frac{\gamma_{\rm v}}{T}\nabla T. \tag{41}$$

Because the annihilation of vortices requires a finite excitation energy, $\gamma_{\rm v}$ vanishes quickly at $T = 0$; therefore, the force will vanish at $T = 0$. It would be interesting to experimentally study whether the direct thermal force does or does not exist.

IX. LINEAR RESPONSE THEORY OF MAGNON CURRENT

We calculate the magnon current induced by the temperature gradient within the linear response theory using the nonequilibrium Green's function. (Standard Kubo formula calculation is also applicable.) The interaction H_{A_T} in the Fourier representation of the magnon operators $[b(\boldsymbol{r},t) = \sqrt{\frac{a^3}{V}}\int\frac{d\omega}{2\pi}\sum_{\boldsymbol{q}} e^{i(\boldsymbol{q}\cdot\boldsymbol{r}-\omega t)} b_{\boldsymbol{q},\omega}]$ is given by

$$H_{A_T} = -2JS\int\frac{d\omega}{2\pi}\int\frac{d\Omega}{2\pi}\frac{1}{V}\sum_{\boldsymbol{q}} e^{i\Omega t} q_i\omega \times A_{T,i}(-\Omega) b^{\dagger}_{\boldsymbol{q},\omega+\frac{\Omega}{2}} b_{\boldsymbol{q},\omega-\frac{\Omega}{2}}, \tag{42}$$

where Ω is an infinitesimal external angular frequency and V is the system volume. The "paramagnetic" and "diamagnetic" magnon currents described by Eqs. (19) and (22), respectively, are

$$j^{(0)}_{{\rm m},i} = i\int\frac{d\omega}{2\pi}\int\frac{d\Omega}{2\pi}\frac{1}{V}\sum_{\boldsymbol{q}} e^{i\Omega t} q_i G^<_{\boldsymbol{q},\omega-\frac{\Omega}{2},\boldsymbol{q},\omega+\frac{\Omega}{2}},$$
$$j^{(\rm d)}_{{\rm m},i} = -i\int\frac{d\omega}{2\pi}\int\frac{d\Omega}{2\pi}\frac{1}{V}\sum_{\boldsymbol{q}} e^{i\Omega t}\omega A_{T,i}(-\Omega) G^<_{\boldsymbol{q},\omega-\frac{\Omega}{2},\boldsymbol{q},\omega+\frac{\Omega}{2}}, \tag{43}$$

where $G^<_{\boldsymbol{q},\omega,\boldsymbol{q}',\omega'} \equiv -i\langle b^{\dagger}_{\boldsymbol{q}'\omega'} b_{\boldsymbol{q}\omega}\rangle$ is the lesser component of the nonequilibrium Green's function of magnons [59]. The "paramagnetic" contribution is calculated at the linear order in H_{A_T} as

$$j^{(0)}_{{\rm m},i} = -i\frac{2JS}{V}\int\frac{d\omega}{2\pi}\int\frac{d\Omega}{2\pi}\sum_{\boldsymbol{q}} q_i q_j \omega\left[g_{\boldsymbol{q},\omega-\frac{\Omega}{2}} g_{\boldsymbol{q},\omega+\frac{\Omega}{2}}\right]^<, \tag{44}$$

where $g_{\boldsymbol{q}\omega}$ denotes the free nonequilibrium Green's function. The lesser Green's function is written in terms of retarded and advanced Green's functions as follows [60]:

$$\begin{aligned}\left[g_{\boldsymbol{q},\omega-\frac{\Omega}{2}} g_{\boldsymbol{q},\omega+\frac{\Omega}{2}}\right]^< &= \left[n\left(\omega+\frac{\Omega}{2}\right) - n\left(\omega-\frac{\Omega}{2}\right)\right] g^{\rm r}_{\boldsymbol{q},\omega-\frac{\Omega}{2}} g^{\rm a}_{\boldsymbol{q},\omega+\frac{\Omega}{2}} \\ &\quad - n\left(\omega+\frac{\Omega}{2}\right) g^{\rm r}_{\boldsymbol{q},\omega-\frac{\Omega}{2}} g^{\rm r}_{\boldsymbol{q},\omega+\frac{\Omega}{2}} \\ &\quad + n\left(\omega-\frac{\Omega}{2}\right) g^{\rm a}_{\boldsymbol{q},\omega-\frac{\Omega}{2}} g^{\rm a}_{\boldsymbol{q},\omega+\frac{\Omega}{2}} \\ &\simeq n(\omega)\left[\left(g^{\rm a}_{\boldsymbol{q},\omega}\right)^2 - \left(g^{\rm r}_{\boldsymbol{q},\omega}\right)^2\right] - \frac{\Omega}{2} n'(\omega)\left(g^{\rm a}_{\boldsymbol{q},\omega} - g^{\rm r}_{\boldsymbol{q},\omega}\right)^2,\end{aligned} \tag{45}$$

where $n(\omega) \equiv [e^{\beta\omega} - 1]^{-1}$ is the Bose distribution function, $n'(\omega) \equiv \frac{dn}{d\omega}$, $\beta \equiv 1/(k_B T)$ (k_B is the Boltzmann constant), and we have neglected contribution of the order of Ω^2. The retarded and advanced Green's functions are

$$g^{\rm r}_{\boldsymbol{q}\omega} = \frac{1}{\omega - \omega_q + i\alpha\omega}, \tag{46}$$

and $g^{\rm a}_{\boldsymbol{q}\omega} = (g^{\rm r}_{\boldsymbol{q}\omega})^*$, where ω_q is the angular frequency of the magnon with a wave vector $\boldsymbol{q}$ and the effect of Gilbert damping is included as an imaginary part. Thus, the "paramagnetic" magnon current is

$$\begin{aligned} j^{(0)}_{{\rm m},i} &= JS\int\frac{d\omega}{2\pi}\int\frac{d\Omega}{2\pi}\frac{1}{V}\sum_{\boldsymbol{q}} q_i q_j (i\Omega) \\ &\quad \times A_{T,j}(-\Omega)\omega n'(\omega)\left(g^{\rm a}_{\boldsymbol{q}\omega} - g^{\rm r}_{\boldsymbol{q}\omega}\right)^2 \\ &\quad + i\int\frac{d\omega}{2\pi}\int\frac{d\Omega}{2\pi}\frac{1}{V}\sum_{\boldsymbol{q}} A_{T,i}(-\Omega)\omega n(\omega)\left(g^{\rm a}_{\boldsymbol{q}\omega} - g^{\rm r}_{\boldsymbol{q}\omega}\right),\end{aligned} \tag{47}$$

where we used $2JSq_j(g^{\rm a}_{\boldsymbol{q}\omega})^2 = \partial_{q_j} g^{\rm a}_{\boldsymbol{q}\omega}$. Similarly, the "diamagnetic" magnon current is calculated as follows:

$$\boldsymbol{j}^{(\rm d)}_{\rm m} = -i\int\frac{d\omega}{2\pi}\int\frac{d\Omega}{2\pi}\frac{1}{V}\sum_{\boldsymbol{q}} A_{T,i}(-\Omega)\omega n(\omega)\left(g^{\rm a}_{\boldsymbol{q}\omega} - g^{\rm r}_{\boldsymbol{q}\omega}\right). \tag{48}$$

We see that the "diamagnetic" current cancels an equilibrium contribution of the "paramagnetic" current, resulting in (assuming rotational symmetry and using $\int\frac{d\Omega}{2\pi}(-i\Omega)A_{T,i}(-\Omega) = \dot{\boldsymbol{A}}_T = \frac{\nabla T}{T}$)

$$j_{{\rm m},i} = -\kappa\nabla_i T, \tag{49}$$

where the coefficient κ is

$$\begin{aligned}\kappa &= \frac{JS}{3\hbar}\frac{1}{T}\int\frac{d\omega}{2\pi}\frac{1}{V}\sum_{\boldsymbol{q}} q^2\omega n'(\omega)\left(g^{\rm r}_{\boldsymbol{q}\omega} - g^{\rm a}_{\boldsymbol{q}\omega}\right)^2 \\ &= -\frac{4JS}{3\hbar}\alpha^2\frac{1}{T}\frac{1}{V}\sum_{\boldsymbol{q}} q^2\int\frac{d\omega}{2\pi} n'(\omega)\frac{\omega^3}{[(\omega-\omega_q)^2 + (\alpha\omega)^2]^2}.\end{aligned} \tag{50}$$

To evaluate the summation over $\boldsymbol{q}$, we consider the case of uniaxial anisotropy ($K_\perp \ll K$) for simplicity. Then, the magnon energy is $\hbar\omega_q = JSq^2 + \Delta_{\rm sw}$, where $\Delta_{\rm sw} = KS$ is the gap of spin wave. The summation over $\boldsymbol{q}$ is performed in three dimensions, and by defining $\epsilon \equiv JSq^2 + \Delta_{\rm sw}$, we obtain

$$\begin{aligned}&\frac{1}{V}\sum_{\boldsymbol{q}} q^2\frac{1}{[(\omega-\omega_q)^2 + (\alpha\omega)^2]^2} \\ &\quad = \frac{1}{4\pi^2(JS)^{5/2}}\int_{\Delta_{\rm sw}}^{\infty} d\epsilon(\epsilon - \Delta_{\rm sw})^{3/2}\frac{1}{[(\epsilon-\omega)^2 + (\alpha\omega)^2]^2} \\ &\quad = \frac{1}{2\pi(JS)^{5/2}\alpha^3}\theta(\omega - \Delta_{\rm sw})\frac{(\omega - \Delta_{\rm sw})^{3/2}}{\omega^3},\end{aligned} \tag{51}$$

where $\theta(x)$ is the step function and we used an approximation (using $\alpha \ll 1$)

$$\frac{1}{[(\epsilon-\omega)^2 + (\alpha\omega)^2]^2} \simeq \frac{2\pi}{(\alpha\omega)^3}\delta(\epsilon - \omega). \tag{52}$$

Thus, the result is

$$\kappa = -\frac{1}{3\pi^2 (JS)^{3/2}} \frac{1}{\alpha T} \int_{\Delta_{\rm sw}}^{\infty} d\omega (\omega - \Delta_{\rm sw})^{3/2} \frac{dn(\omega)}{d\omega} = \frac{1}{2\pi^2 (JS)^{3/2}} \frac{1}{\alpha} k_B (k_B T)^{1/2} F(\beta\Delta_{\rm sw}), \quad (53)$$

where

$$F(\beta\Delta_{\rm sw}) \equiv \int_{\beta\Delta_{\rm sw}}^{\infty} dx \frac{(x-\beta\Delta_{\rm sw})^{1/2}}{e^x - 1}. \quad (54)$$

At high temperatures, $\beta\Delta_{\rm sw} \ll 1$, $F = 2.315$. Note that the thermal transport coefficients are proportional to the damping time constant, α^{-1}, in the same manner as in the electric transport coefficients in metals are proportional to the elastic lifetime, τ. The obtained result, $\kappa \propto \sqrt{T}/\alpha$, agrees with the semiclassical calculation in the supplementary information of Ref. [11].

X. DOMAIN WALL SOLUTION

Using the result for the magnon current given by Eqs. (49) and (53), the equation of motion for a domain wall [Eq. (30)] is expressed as follows:

$$\dot{\phi} + \alpha\frac{\dot{X}}{\lambda} = \beta_T \frac{u_T}{\lambda}, \quad (55)$$

$$\dot{X} - \alpha\lambda\dot{\phi} = v_{\rm c} \sin 2\phi - P_T u_T, \quad (56)$$

where

$$v_{\rm c} \equiv \frac{K_\perp \lambda S}{2\hbar}, \quad (57)$$

and

$$u_T \equiv -\frac{k_B a^2}{\hbar} \nabla_z T \quad (58)$$

represents the scale of the velocity induced by the temperature gradient (with positive direction chosen as the direction from the high- to the low-temperature region). The spin-polarization coefficient in the thermal magnon spin-transfer depends on the temperature according to

$$P_T \equiv \frac{2J\kappa}{k_B a^2} = \frac{F}{\pi^2\sqrt{S}} \frac{1}{\alpha} \sqrt{k_B T \frac{a^2}{JS^2}}, \quad (59)$$

where $F = 2.315$ considering the high temperature ($\beta\Delta_{\rm sw} \ll 1$). Note that there is a minus sign in the magnon spin-transfer term (proportional to P_T) in Eq. (30), indicating that the magnon spin-transfer pushes the wall to the hotter end of the system as has been noted previously [12,13]. Equation (59) indicates a clear distinction between the magnon spin-transfer effect and the electron spin-transfer effect in metals, namely, the spin-transfer efficiency parameter, P_T, grows at small damping (α); however, this parameter is independent of α in the case of electron spin-transfer effect.

The equation of motion [Eq. (30)] has the same form as in the current-driven case in metals. As was shown in Ref. [20], the wall shows distinctly different behaviors at small and large values of u_T compared to the crossover velocity (Walker's breakdown velocity), defined as

$$u_{\rm c} \equiv -\frac{v_{\rm c}}{P_T + \frac{\beta_T}{\alpha}}, \quad (60)$$

which depends on the temperature and α. At a small driving velocity, $|u_T| \leqslant |u_{\rm c}|$, the tilting angle of the wall, ϕ, reaches the terminal angle determined by

$$\sin 2\phi = \left(P_T + \frac{\beta_T}{\alpha}\right)\frac{u_T}{v_{\rm c}}, \quad (61)$$

and the terminal velocity of the wall is a constant,

$$v_{\rm w} = \frac{\beta_T}{\alpha} u_T. \quad (62)$$

In this case, the wall moves from the high- to low-temperature region because of the pressure on the wall. Above the crossover velocity, $|u_T| > |u_{\rm c}|$, the angle ϕ becomes time-dependent and the average wall velocity is

$$v_{\rm w} = \frac{\beta_T}{\alpha} u_T - \frac{v_{\rm c}}{1+\alpha^2} \sqrt{\left(P_T + \frac{\beta_T}{\alpha}\right)^2 \left(\frac{u_T}{v_{\rm c}}\right)^2 - 1}. \quad (63)$$

For $u_T \gg |u_{\rm c}|$, $v_{\rm w} = \frac{1}{1+\alpha^2}(-P_T + \alpha\beta_T)u_T$. If $P_T - \alpha\beta_T > 0$, the direction of domain wall motion changes around $u_T \sim O(|u_{\rm c}|)$: at small ∇T, the motion is toward the colder end, while the opposite in the case in the region of large ∇T dominated by magnon spin-transfer effect. At $u_T \gg |u_{\rm c}|$, the wall velocity is $v_{\rm w}/\nabla T = -\frac{k_B a^2}{\hbar}(P_T - \alpha\beta_T)$.

The domain wall velocity as a function of $u_T/v_{\rm c}$ is plotted in Fig. 1 for different temperatures and β_T. When there is no force ($\beta_T = 0$), there is a threshold value of $\frac{v_{\rm c}}{P_T}$ for u_T for thermal motion to set in, and the motion toward the hotter region occurs above the threshold. The wall speed increases as function of the temperature because the effective spin polarization, P_T,

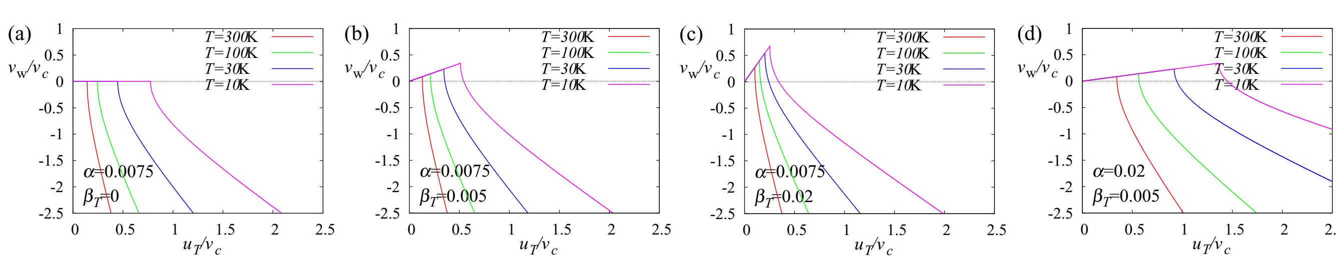

FIG. 1. (Color online) (a)–(c) The domain wall velocity [Eq. (63)] in the unit of $v_{\rm c}$ as a function of $u_T/v_{\rm c}$ for different temperatures and for $\beta_T = 0, 0.005$ and 0.02 at $\alpha = 0.0075$. Negative $v_{\rm w}$ is toward the direction of the hotter side. $a = 12$ Å, $S = 14$, $\frac{JS^2}{a^2 k_B} = 4.2 \times 10^2$ K are used. The case of $\alpha = 0.02$ with $\beta_T = 0.005$ is plotted in panel (d). Effects of extrinsic pinning are not considered. At high temperature, it is seen that the magnon spin-transfer effect is enhanced for small α.

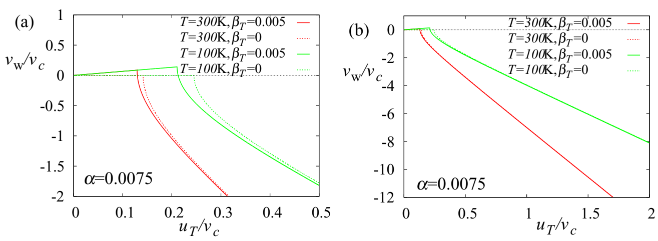

FIG. 2. (Color online) The domain wall velocity for $\beta_T = 0$ and $\beta = 0.005$ at $T = 100$ K and 300 K at $\alpha = 0.0075$ for (a) small and (b) large u_T/v_c. We see that dependence of the domain wall velocity on β_T is weak.

increases at high temperatures rather significantly ($\propto\sqrt{T}$). If β_T is positive as was reported in Ref. [24], wall motion toward the colder regime occurs at small $u_T(<|u_c|)$, and the magnon spin-transfer regime appears at $|u_T| \gtrsim |u_c|$. For large α, the wall speed is smaller [Fig. 1(d)].

In YIG, $\alpha = 0.0075$, $a = 12$ Å, and the magnetization is $M = 1.4 \times 10^5$ A/m. If we convert the magnetization to the average magnitude of spin using $M = \frac{2\mu_B}{a^3}S$, we find that the effective spin S is equal to 14. The exchange stiffness is $A = 4.7 \times 10^{-12}$ J/m, which corresponds to $\frac{JS^2}{a^2} = Aa = 5.8 \times 10^{-21}$ J ($\frac{JS^2}{a^2 k_B} = 4.2 \times 10^2$ K). Therefore, for the three-dimensional case, we obtain $P_T = 0.40 \times \sqrt{T(\mathrm{K})}$. (At $T = 300$ K, $P_T = 6.7$ and the crossover velocity is $u_c = -v_c \times 0.15$.) The absolute value of the wall speed depends on the hard-axis anisotropy energy $K_\perp$ ($v_c \propto K_\perp$). The easy-axis anisotropy energy of YIG is $KS^2a^3 = 1.2 \times 10^{-24}$ J, and the hard-axis energy is much lesser than the easy-axis energy. Let us select $K_\perp/K = 10^{-3}$, i.e., $v_c = 2.4 \times 10^{-2}$ m/s. We consider the case of $\beta_T = 0$ first. Here, $|u_c| = 0.36 \times 10^{-2}$ m/s at $T = 300$ K. In this case, a temperature gradient $\nabla T = 20$ K/mm in Ref. [11] corresponds to $u_T = 3.8 \times 10^{-3}$ m/s ($u_T/v_c = 0.16$) and is close to the threshold ($u_T \simeq |u_c|$); the wall speed is then obtained from Figs. 1(a) and 2(a) as $v_w = -0.37v_c = -0.89 \times 10^{-2}$ m/s. In the case of $\beta_T = 0.005$, $u_T/v_c = 0.16$ leads to $v_w = -0.50v_c = -1.2 \times 10^{-2}$ m/s [Figs. 1(b) and 2(a)], and we see that the order of magnitude of the speed does not depend strongly on β_T [Fig. 2(a)]. Interestingly, the wall velocity changes sign as the temperature is lowered if β_T is a positive constant. In fact, when we set $u_T/v_c = 0.16$ for $\beta_T = 0.005$, the wall velocity is negative at $T = 300$ K, while it is positive at $T = 100$ K as seen in Fig. 2(a). The sign change occurs around $T = 190$ K, where $u_c(T) \sim u_T$.

If hard-axis anisotropy is weaker, $K_\perp/K = 10^{-4}, v_w = -11v_c = -2.6 \times 10^{-2}$ m/s at $T = 300$ K and $v_w = -6v_c = -1.4 \times 10^{-2}$ m/s at $T = 100$ K for $u_T = 3.8 \times 10^{-3}$ m/s for both $\beta_T = 0$ and 0.005 [Fig. 2(b)].

In the experiment on YIG at room temperature in Ref. [11], the wall moved to the hotter region at the speed of 1.8×10^{-4} m/s for $\nabla T = 22$ K/mm. This is slower by two orders of magnitude than our theoretical estimate, and we suspect that the small value is caused by extrinsic pinning. In fact, the experiment was performed under a rather strong field of $B = 6 \times 10^{-3}$ T (60 Oe), which adds a large additional force term $\frac{g\mu_B B}{\hbar} = 1 \times 10^9$ s^{-1} to the right-hand side of Eq. (55). This force is expected to have been necessary to compensate for the extrinsic pinning effects, and this fact and the observed avalanche behavior of the walls suggest a strong influence of extrinsic pinning in their sample.

In the experiment performed in metals in Ref. [15], the applied ∇T was of the order of 100 K/mm. The motion was observed in the presence of an ac magnetic field to remove the extrinsic pinning effects and a wall velocity of 2 mm/s toward the colder end was obtained. The direction of the motion can be explained by the spin-transfer effect of the thermally induced conduction electron flow.

XI. CONCLUSION

To summarize, we applied a thermal vector potential theory developed in Ref. [45] to describe magnetization dynamics in a ferromagnetic insulator driven by a temperature gradient. We evaluated the magnon current induced by the temperature gradient within the linear response theory and found that it is proportional to the inverse of the Gilbert damping parameter. Thus, the effect of the magnon current is dominant in weak damping systems as was argued in Ref. [22]. The magnon current was demonstrated to exert a spin-transfer torque on a domain wall, and this effect tends to drive the structure toward the hotter side. The case of a vortex (or a skyrmion) was also discussed.

ACKNOWLEDGMENTS

The author thanks H. Kohno and S.-K. Kim for valuable discussions. This work was supported by a Grant-in-Aid for Scientific Research (C) (Grant No. 25400344), (A) (Grant No. 24244053) from Japan Society for the Promotion of Science and Grant-in-Aid for Scientific Research on Innovative Areas (Grant No. 26103006) from The Ministry of Education, Culture, Sports, Science and Technology (MEXT), Japan.

APPENDIX: ENERGY CURRENT DENSITY OF LOCALIZED SPIN

Here, we derive the expression for the energy current density of the localized spin by quantum mechanically evaluating the time-derivative of the energy density. We consider a Hamiltonian with exchange interaction and easy- and hard-axis anisotropy energies [Eq. (5)]. We perform the calculation on a discretized lattice, because this allows a straightforward estimation of the commutators, and then take the continuum limit. The energy densities at site i are

$$\mathcal{E}_i^J \equiv -\frac{J}{2a^5}\sum_{\alpha\beta}\sum_{\sigma=\pm} S_i^\alpha S_{i+\sigma\beta}^\alpha,$$
$$\mathcal{E}_i^K \equiv -\frac{K}{2a^3}(S_i^z)^2, \quad \mathcal{E}_i^{K_\perp} \equiv \frac{K_\perp}{2a^3}(S_i^y)^2, \tag{A1}$$

where α,β runs over x, y, and z, and σ denotes the positive and negative directions. The corresponding terms of the discretized Hamiltonian are

$$H_J \equiv a^3\sum_i \mathcal{E}_i^J, \quad H_K \equiv a^3\sum_i \mathcal{E}_i^K, \quad H_{K_\perp} \equiv a^3\sum_i \mathcal{E}_i^{K_\perp}. \tag{A2}$$

We first study the exchange interaction contribution by evaluating $[\mathcal{E}_i^J, H_J]$;

$$\left[\mathcal{E}_i^J, H_J\right] = \frac{J^2}{4a^7} \sum_j \sum_{\alpha\alpha'\beta\beta'} \sum_{\sigma\sigma'} \left[S_i^\alpha S_{i+\sigma\beta}^\alpha, S_j^{\alpha'} S_{j+\sigma'\beta'}^{\alpha'}\right]. \tag{A3}$$

Using $[S_i^\alpha, S_j^\beta] = i\delta_{ij}\epsilon_{\alpha\beta\gamma}S_i^\gamma$ and

$$[AB,CD] = A[B,C]D + [A,C]BD + CA[B,D] + C[A,D]B, \tag{A4}$$

we observe that

$$\begin{aligned}\sum_j \left[S_i^\alpha S_{i+\sigma\beta}^\alpha, S_j^{\alpha'} S_{j+\sigma'\beta'}^{\alpha'}\right] &= i \sum_\delta \epsilon_{\alpha\alpha'\delta}\left(S_i^\alpha S_{i+\sigma\beta}^\delta S_{i+\sigma\beta+\sigma'\beta'}^{\alpha'} + S_i^\delta S_{i+\sigma\beta}^\alpha S_{i+\sigma'\beta'}^{\alpha'} + S_{i+\sigma\beta-\sigma'\beta'}^{\alpha'} S_i^\alpha S_{i+\sigma\beta}^\delta + S_{i-\sigma'\beta'}^{\alpha'} S_i^\delta S_{i+\sigma\beta}^\alpha\right)\\ &= i \sum_\delta \epsilon_{\alpha\alpha'\delta}\left[-2S_i^\alpha S_{i+\sigma\beta}^{\alpha'}\left(S_{i+\sigma\beta+\sigma'\beta'}^\delta - S_{i+\sigma'\beta'}^\delta\right) + \sum_\epsilon \epsilon_{\alpha\alpha'\epsilon}\left(\delta_{\sigma\beta,\sigma'\beta'} S_i^\epsilon S_{i+\sigma\beta}^\delta - \delta_{\sigma\beta,-\sigma'\beta'} S_i^\delta S_{i+\sigma\beta}^\epsilon\right)\right],\end{aligned} \tag{A5}$$

where the fact that spins on different sites commute with each other was used. The contributions from the last two terms vanish after summation over σ and σ', and we obtain

$$\left[\mathcal{E}_i^J, H_J\right] = -i\frac{J^2}{2a^7} \sum_{\alpha\alpha'\beta\beta'\delta} \sum_{\sigma,\sigma'=\pm} \epsilon_{\alpha\alpha'\delta} S_i^\alpha S_{i+\sigma\beta}^{\alpha'}\left(S_{i+\sigma\beta+\sigma'\beta'}^\delta - S_{i+\sigma'\beta'}^\delta\right). \tag{A6}$$

The commutators including the exchange interaction and easy-axis anisotropy energy are

$$\left[\mathcal{E}_i^J, H_K\right] + \left[\mathcal{E}_i^K, H_J\right] = -i\frac{JK}{4a^5} \sum_{\alpha\alpha'\beta} \sum_{\sigma=\pm} \epsilon_{\alpha\alpha'z}\left[S_i^\alpha S_{i+\sigma\beta}^{\alpha'} S_{i+\sigma\beta}^z + S_{i+\sigma\beta}^z S_i^\alpha S_{i+\sigma\beta}^{\alpha'} - S_{i+\sigma\beta}^\alpha S_i^{\alpha'} S_i^z - S_i^z S_{i+\sigma\beta}^\alpha S_i^{\alpha'}\right]. \tag{A7}$$

The hard-axis anisotropy contribution has the same form but with the index z replaced by y.

Let us consider the continuum limit. Contribution from the exchange interaction is ($\mu = x, y, z$)

$$\left[\mathcal{E}_i^J, H_J\right] = i\frac{J^2}{2a^3} \sum_{\alpha\alpha'\beta\delta} \sum_{\sigma=\pm} \epsilon_{\alpha\alpha'\delta}(\sigma\nabla_\beta S^\alpha) S^{\alpha'} \sigma\nabla_\beta(\nabla^2 S^\delta) = -i\hbar\nabla\cdot\boldsymbol{j}_\mathcal{E}^{JJ}, \tag{A8}$$

where

$$j_{\mathcal{E},\mu}^{JJ} \equiv \frac{J^2}{\hbar a^3}\{\nabla_\mu \boldsymbol{S}\cdot[(\nabla^2\boldsymbol{S})\times\boldsymbol{S}]\} \tag{A9}$$

is the energy current from the exchange interaction. Similarly,

$$\left[\mathcal{E}_i^J, H_K\right] + \left[\mathcal{E}_i^K, H_J\right] = -i\hbar\nabla\cdot\boldsymbol{j}_\mathcal{E}^{JK}, \quad \left[\mathcal{E}_i^J, H_{K_\perp}\right] + \left[\mathcal{E}_i^{K_\perp}, H_J\right] = -i\hbar\nabla\cdot\boldsymbol{j}_\mathcal{E}^{JK_\perp}, \tag{A10}$$

where

$$\begin{aligned}\boldsymbol{j}_{\mathcal{E},\mu}^{JK} &\equiv \frac{JK}{4\hbar a^3}[(\boldsymbol{S}\times\nabla_\mu\boldsymbol{S} - \nabla_\mu\boldsymbol{S}\times\boldsymbol{S})_z S_z + S_z(\boldsymbol{S}\times\nabla_\mu\boldsymbol{S} - \nabla_\mu\boldsymbol{S}\times\boldsymbol{S})_z],\\ \boldsymbol{j}_{\mathcal{E},\mu}^{JK_\perp} &\equiv -\frac{JK_\perp}{4\hbar a^3}[(\boldsymbol{S}\times\nabla_\mu\boldsymbol{S} - \nabla_\mu\boldsymbol{S}\times\boldsymbol{S})_y S_y + S_y(\boldsymbol{S}\times\nabla_\mu\boldsymbol{S} - \nabla_\mu\boldsymbol{S}\times\boldsymbol{S})_y].\end{aligned} \tag{A11}$$

In the classical case, where ordering does not matter, we obtain

$$\begin{aligned}\boldsymbol{j}_{\mathcal{E},\mu}^{JK} &= \frac{JK}{\hbar a^3}(\boldsymbol{S}\times\nabla_\mu\boldsymbol{S})_z S_z = -\gamma\frac{J}{a^3}\nabla_\mu\boldsymbol{S}\cdot(\boldsymbol{B}_K\times\boldsymbol{S}),\\ \boldsymbol{j}_{\mathcal{E},\mu}^{JK_\perp} &= -\gamma\frac{J}{a^3}\nabla_\mu\boldsymbol{S}\cdot(\boldsymbol{B}_{K_\perp}\times\boldsymbol{S}),\end{aligned} \tag{A12}$$

where γ is the gyromagnetic ratio, and

$$\begin{aligned}\hbar\gamma\boldsymbol{B}_K &\equiv -KS_z\hat{\boldsymbol{z}},\\ \hbar\gamma\boldsymbol{B}_{K_\perp} &\equiv K_\perp S_y\hat{\boldsymbol{y}}\end{aligned} \tag{A13}$$

are the effective magnetic fields for the easy and hard-axis anisotropy energies, respectively ($\hat{\boldsymbol{y}}$ and $\hat{\boldsymbol{z}}$ are the unit vectors along y and z axis, respectively). There is no contribution to the energy current from the commutators of the anisotropy energies because local quantities commute with each other. Therefore, the total energy current associated with the Hamiltonian Eq. (5) is

$$\begin{aligned}\boldsymbol{j}_{\mathcal{E},\mu} &\equiv \boldsymbol{j}_{\mathcal{E},\mu}^{JJ} + \boldsymbol{j}_{\mathcal{E},\mu}^{JK} + \boldsymbol{j}_{\mathcal{E},\mu}^{JK_\perp}\\ &= -\gamma\frac{J}{a^3}\nabla_\mu\boldsymbol{S}\cdot(\boldsymbol{B}_H\times\boldsymbol{S}),\end{aligned} \tag{A14}$$

where

$$\hbar\gamma \boldsymbol{B}_H \equiv \frac{\delta H}{\delta \boldsymbol{S}} = -J\nabla^2 \boldsymbol{S} - K S_z \hat{\boldsymbol{z}} + K_\perp S_y \hat{\boldsymbol{y}} \tag{A15}$$

is the total effective magnetic field for the Hamiltonian H. The equation of motion for $\boldsymbol{S}$ is

$$\dot{\boldsymbol{S}} = \gamma \boldsymbol{B}_H \times \boldsymbol{S}, \tag{A16}$$

and thus we finally obtain the energy current density as

$$\boldsymbol{j}_{\mathcal{E},\mu} = -\frac{J}{a^3}\nabla_\mu \boldsymbol{S}\cdot\dot{\boldsymbol{S}}. \tag{A17}$$

This form is identical to the form obtained from a general definition in terms of the Lagrangian $L, T_{0i} \equiv (\partial_t \boldsymbol{S})\frac{\delta L}{\delta \partial_i \boldsymbol{S}}$. It also agrees with the form proposed in Ref. [28] based on a symmetry argument, although the spin relaxation was believed there to be essential for the emergence of the form of Eq. (A17).

[1] L. Berger, Phys. Rev. B **33**, 1572 (1986).
[2] L. Berger, Phys. Rev. B **54**, 9353 (1996).
[3] J. C. Slonczewski, J. Magn. Magn. Mater. **159**, L1 (1996).
[4] E. Saitoh, M. Ueda, H. Miyajima, and G. Tatara, Appl. Phys. Lett. **88**, 182509 (2006).
[5] T. Kimura, Y. Otani, T. Sato, S. Takahashi, and S. Maekawa, Phys. Rev. Lett. **98**, 156601 (2007).
[6] Y. Kajiwara *et al.*, Nature **464**, 262 (2010).
[7] K. Uchida, S. Takahashi, K. Harii, J. Ieda, W. Koshibae, K. Ando, S. Maekawa, and E. Saitoh, Nature **455**, 778 (2008).
[8] K. Uchida, H. Adachi, T. An, T. Ota, M. Toda, B. Hillebrands, S. Maekawa, and E. Saitoh, Nat Mater **10**, 737 (2011).
[9] M. Hatami, G. E. W. Bauer, Q. Zhang, and P. J. Kelly, Phys. Rev. Lett. **99**, 066603 (2007).
[10] A. Kirihara, K.-i. Uchida, Y. Kajiwara, M. Ishida, Y. Nakamura, T. Manako, E. Saitoh, and S. Yorozu, Nat. Mater. **11**, 686 (2012).
[11] W. Jiang *et al.*, Phys. Rev. Lett. **110**, 177202 (2013).
[12] D. Hinzke and U. Nowak, Phys. Rev. Lett. **107**, 027205 (2011).
[13] P. Yan and G. E. W. Bauer, Phys. Rev. Lett. **109**, 087202 (2012).
[14] X. S. Wang and X. R. Wang, Phys. Rev. B **90**, 014414 (2014).
[15] S. U. Jen and L. Berger, J. Appl. Phys. **59**, 1285 (1986).
[16] L. Berger, J. Appl. Phys. **58**, 450 (1985).
[17] S. U. Jen and L. Berger, J. Appl. Phys. **59**, 1278 (1986).
[18] K. M. Hals, A. Brataas, and G. E. Bauer, Solid State Commun. **150**, 461 (2010).
[19] A. Thiaville, Y. Nakatani, J. Miltat, and Y. Suzuki, Europhys. Lett. **69**, 990 (2005).
[20] G. Tatara, T. Takayama, H. Kohno, J. Shibata, Y. Nakatani, and H. Fukuyama, J. Phys. Soc. Japan **75**, 064708 (2006).
[21] G. Tatara, H. Kohno, and J. Shibata, Phys. Rep. **468**, 213 (2008).
[22] L. Kong and J. Zang, Phys. Rev. Lett. **111**, 067203 (2013).
[23] A. A. Kovalev, Phys. Rev. B **89**, 241101 (2014).
[24] S. K. Kim and Y. Tserkovnyak, Phys. Rev. B **92**, 020410(R) (2015).
[25] F. Schlickeiser, U. Ritzmann, D. Hinzke, and U. Nowak, Phys. Rev. Lett. **113**, 097201 (2014).
[26] P. Yan, Y. Cao, and J. Sinova, arXiv:1504.00651 (2015).
[27] G. Tatara and H. Kohno, Phys. Rev. Lett. **92**, 086601 (2004).
[28] A. A. Kovalev and Y. Tserkovnyak, Europhys. Lett. **97**, 67002 (2012).
[29] J. M. Luttinger, Phys. Rev. **135**, A1505 (1964).
[30] L. Smrcka and P. Streda, J. Phys. C: Solid State Phys. **10**, 2153 (1977).
[31] H. Oji and P. Streda, Phys. Rev. B **31**, 7291 (1985).
[32] N. R. Cooper, B. I. Halperin, and I. M. Ruzin, Phys. Rev. B **55**, 2344 (1997).
[33] G. Catelani and I. Aleiner, J. Exp. Theoret. Phys. **100**, 331 (2005).
[34] K. Michaeli and A. M. Finkel'stein, Phys. Rev. B **80**, 115111 (2009).
[35] T. Qin, Q. Niu, and J. Shi, Phys. Rev. Lett. **107**, 236601 (2011).
[36] G. Schwiete and A. M. Finkel'stein, Phys. Rev. B **90**, 060201 (2014).
[37] F. G. Eich, M. Di Ventra, and G. Vignale, Phys. Rev. Lett. **112**, 196401 (2014).
[38] F. G. Eich, A. Principi, M. Di Ventra, and G. Vignale, Phys. Rev. B **90**, 115116 (2014).
[39] R. Matsumoto and S. Murakami, Phys. Rev. Lett. **106**, 197202 (2011).
[40] R. Matsumoto and S. Murakami, Phys. Rev. B **84**, 184406 (2011).
[41] R. Matsumoto, R. Shindou, and S. Murakami, Phys. Rev. B **89**, 054420 (2014).
[42] H. Kohno, Y. Hiraoka, M. Hatami, and G. E. W. Bauer, arXiv:1408.4562 (2014).
[43] P. N. Butcher, J. Phys.: Cond. Matter **2**, 4869 (1990).
[44] Y. Takezoe, K. Hosono, A. Takeuchi, and G. Tatara, Phys. Rev. B **82**, 094451 (2010).
[45] G. Tatara, Phys. Rev. Lett. **114**, 196601 (2015).
[46] M. Heuser and J. Hajdu, Zeitschrift für Physik **270**, 289 (1974).
[47] A. Shitade, Progr. Theoret. Exp. Phys. **2014**, 123I01 (2014).
[48] R. Utiyama, Phys. Rev. **101**, 1597 (1956).
[49] D. Miura and A. Sakuma, J. Phys. Soc. Japan **81**, 113602 (2012).
[50] This continuity equation holds when the condition of local equilibrium is satisfied.
[51] A. A. Thiele, Phys. Rev. Lett. **30**, 230 (1973).
[52] C. Kittel, *Quantum Theory of Solids* (Wiley, New York, 1963).
[53] We cannot apply Eq. (28) for $T \to 0$, since the assumption of linear response (small perturbation) breaks down.
[54] P. Yan, X. S. Wang, and X. R. Wang, Phys. Rev. Lett. **107**, 177207 (2011).
[55] Y. Le Maho, J.-V. Kim, and G. Tatara, Phys. Rev. B **79**, 174404 (2009).
[56] P. Yan, A. Kamra, Y. Cao, and G. E. W. Bauer, Phys. Rev. B **88**, 144413 (2013).
[57] J. Shibata, Y. Nakatani, G. Tatara, H. Kohno, and Y. Otani, Phys. Rev. B **73**, 020403 (2006).
[58] A. Auerbach, *Intracting Electrons and Quantum Magnetism* (Springer Verlag, Berlin, 1994).
[59] L. P. Kadanoff and G. Baym, *Quantum Statistical Mechanics*, Advanced Books Classics (Westview Press, Boulder, CO, 1994).
[60] H. Haug and A.-P. Jauho, *Quantum Kinetics in Transport and Optics of Semiconductors* (Springer-Verlag, Berlin, 2007).